THE JOURNAL OF BIOLOGICAL CHEMISTRY
Vol. 277, No. 33, Issue of August 16, pp. 30315–30324, 2002

Printed in U.S.A.

Mechanisms Underlying the Neuronal Calcium Sensor-1-evoked Enhancement of Exocytosis in PC12 Cells*

Received for publication, February 4, 2002, and in revised form, April 23, 2002
Published, JBC Papers in Press, May 28, 2002, DOI 10.1074/jbc.M201132200

Schuichi Koizumi‡§, Patrizia Rosa¶, Gary B. Willars‖, R. A. John Challiss‖, Elena Taverna¶, Maura Francolini¶, Martin D. Bootman, Peter Lipp**, Kazuhide Inoue‡, John Roder‡‡, and Andreas Jeromin‡‡§§**

*From the ‡Section of Neuropharmacology, Division of Pharmacology, National Institute of Health Sciences, 1-18-1 Kamiyoga, Setagaya, Tokyo 158-8501, Japan, ¶Institute of Neuroscience, Cellular and Molecular Pharmacology, Department of Pharmacology, 20129 Milano, Italy, the ‖Department of Cell Physiology and Pharmacology, University of Leicester, University Road, Leicester LE1 9HN, United Kingdom, the **Laboratory of Molecular Signalling, The Babraham Institute, Babraham Hall, Cambridge CB2 4AT, United Kingdom, and the ‡‡Samuel Lunenfeld Research Institute, Mount Sinai Hospital, Toronto, Ontario M5G 1X5, Canada*

Neuronal calcium sensor-1 (NCS-1) or the originally identified homologue frequenin belongs to a superfamily of EF-hand calcium binding proteins. Although NCS-1 is thought to enhance synaptic efficacy or exocytosis mainly by activating ion channel function, the detailed molecular basis for the enhancement is still a matter of debate. Here, mechanisms underlying the NCS-1-evoked enhancement of exocytosis were investigated using PC12 cells overexpressing NCS-1. NCS-1 was found to have a broad distribution in the cells being partially distributed in the cytosol and associated to vesicles and tubular-like structures. Biochemical and immunohistochemical studies indicated that NCS-1 partially colocalized with the light synaptic vesicle marker synaptophysin. When stimulated with UTP or bradykinin, agonists to phospholipase C-linked receptors, NCS-1 enhanced the agonist-mediated elementary and global Ca^{2+} signaling and increased the levels of downstream signals of phosphatidylinositol 4-kinase. NCS-1 enhanced the UTP-evoked exocytosis but not the depolarization-evoked Ca^{2+} responses or exocytosis, suggesting that the enhancement by NCS-1 should involve phospholipase C-linked receptor-mediated signals rather than the Ca^{2+} channels or exocytotic machinery *per se*. Taken together, NCS-1 enhances phosphoinositide turnover, resulting in enhancement of Ca^{2+} signaling and exocytosis. This is a novel regulatory mechanism of exocytosis that might involve the activation of phosphatidylinositol 4-kinase.

EF-hand-containing Ca^{2+}-binding proteins include those of the neuronal calcium sensor family. This family of relatively small proteins (<30 kDa) is expressed in neuronal and neuroendocrine cell types and includes recoverin/S-modulin, visinin, visinin-like protein, neurocalcin, hippocalcin, frequenin, and neuronal Ca^{2+} sensor-1 (NCS-1)[1] (1). Recoverin has a well defined role in signal transduction, regulating rhodopsin phosphorylation by inhibiting rhodopsin kinase (2). However, the functions of the other members of this family are unclear.

Frequenin markedly enhances synaptic efficacy by increasing neurotransmitter release in *Drosophila* (3) and *Xenopus* (4) through unknown mechanisms. Furthermore, the expression of NCS-1 (the mammalian homologue of frequenin) in other secretory cell types such as chromaffin cells suggests a more generalized role in exocytosis (5, 6). In a model of synaptic transmission in PC12 cells, NCS-1 potentiated ATP-mediated exocytosis of dense core granules but did not affect Ca^{2+}-induced exocytosis in permeabilized PC12 cells, suggesting that regulation by NCS-1 may be at the level of signal transduction rather than through direct effects on the exocytotic machinery (5, 6). Although the precise mechanisms for such enhancement remain unknown, recent accumulating evidence suggests that NCS-1 or frequenin could modulate ion channels such as non-L-type (7, 8) and P/Q-type (9) voltage-gated Ca^{2+} channels and A-type K^+ channel (10), which may explain such an increased exocytosis.

In addition to ion channels, NCS-1 and/or frequenin binds to multiple proteins such as G-protein receptor kinase 1 (11, 12) to regulate exocytosis and to substitute for calmodulin (13). Recently, the yeast frequenin, but not vertebrate NCS-1 (14), has been demonstrated to bind to and activate phosphatidylinositol 4-OH kinase, a phosphatidylinositol 4-kinase (PtdIns4K) isoform (1). This class of enzyme is key to the supply of the phospholipase C substrate phosphatidylinositol 4,5-bisphosphate ($PtdIns(4,5)P_2$) and therefore has the potential to regulate phosphoinositide and Ca^{2+} signaling mediated by G-protein-coupled receptors (GPCRs) and receptor tyrosine kinases. The potentiation of this signaling pathway may explain the enhancement of GPCR-mediated vesicle exocytosis by NCS-1.

In the current study, we sought to test this hypothesis by examining the subcellular distribution of NCS-1 and its influence on GPCR-mediated phosphoinositide, elementary and/or

* This work was supported by the Consighia Nationale Ricerche Target Project on Biotechnology (to P. R.) and the Japanese Health Science Foundation (to K. I.). The costs of publication of this article were defrayed in part by the payment of page charges. This article must therefore be hereby marked "*advertisement*" in accordance with 18 U.S.C. Section 1734 solely to indicate this fact.

§ Supported by the Uehara Memorial Foundation and a Grant-in-Aid for Scientific Research in Japan (12780593). To whom correspondence should be addressed: Section of Neuropharmacology, Division of Pharmacology, National Institute of Health Sciences, 1-18-1 Kamiyoga, Setagaya, Tokyo 158-8501 Japan. Tel.: 81-3-3700-1141 (ext. 344); Fax: 81-3-3707-6950; E-mail: skoizumi@nihs.go.jp.

§§ Supported by the Medical Research Council of Canada.

[1] The abbreviations used are: NCS-1, neuronal calcium sensor-1; PtdIns4K, phosphatidylinositol 4-kinase; GPCR, G-protein-coupled receptor; PNS, postnuclear supernatant(s); TRITC, tetramethylrhodamine isothiocyanate; SgII, secretogranin II; HPLC, high performance liquid chromatography; $Ins(1,4,5)P_3$, inositol 1,4,5-trisphosphate; CCE, capacitative Ca^{2+} entry; PLC, phospholipase C; PtdIns, phosphatidylinositol; PtdIns(4)P, phosphatidylinositol 4-phosphate; $PtdIns(4,5)P_2$, phosphatidylinositol 4,5-bisphosphate; $InsP_x$, inositol phosphate.

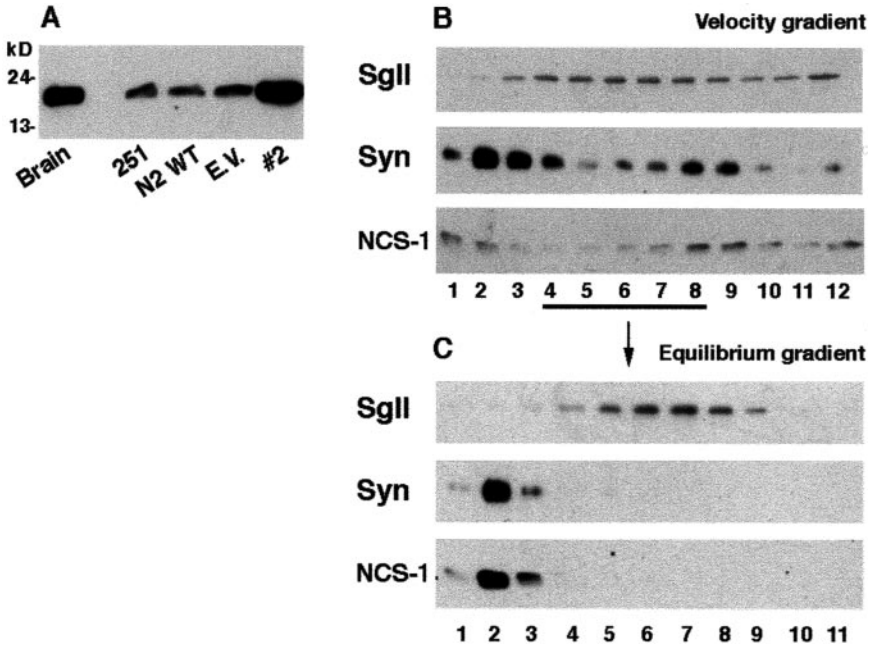

FIG. 1. **Western blotting analysis of NCS-1.** *A*, Western blotting analysis of the PNS (40 mg of proteins) obtained from brain, wild type PC12 cells (clone 251 and N2), and PC12-N2 cells stably transfected with the empty vector (*E.V.*) or cDNA coding for NCS-1 (*#2*) immunolabeled using anti-NCS-1 antibody. *B* and *C*, Western blotting analysis of sucrose gradient fractions obtained as described under "Experimental Procedures." Aliquots containing equivalent amounts of protein were collected from each gradient and pelleted with 80% acetone at −20 °C and analyzed by immunoblotting using antibodies against SgII, synaptophysin (*Syn*), or NCS-1.

global Ca^{2+} signaling, and exocytosis in PC12 cells. The immunolocalization of NCS-1 is consistent with a role for this protein in exocytosis. Further, we demonstrate that NCS-1 enhances UTP- and bradykinin-evoked exocytosis, and this is associated with enhanced agonist-mediated phosphoinositide signaling and potentiated elementary/global Ca^{2+} signaling events. These data suggest that the regulation of a PtdIns4K activity by NCS-1 (1) occurs in mammalian cells and could be the mechanism by which this protein enhances exocytotic responses.

EXPERIMENTAL PROCEDURES

Cell Culture and Generation of NCS-1-overexpressing PC12 Cells—PC12 cells were grown as described previously (15). To establish stable NCS-1 clones, PC12 cells were transfected with the rat *ncs-1* cDNA (GenBank™ accession number L27421) in pClNeo (kindly provided by Jan Eggermont) and selected for neomycin resistance following standard protocols. Stable clones were further characterized by Western blotting and immunofluorescence as described below.

Subcellular Fractionation—NCS-1 cells were subjected to subcellular fractionation as previously described (16, 17) with minor modifications. Briefly, cells were homogenized in buffer containing 0.25 M sucrose, 1 mM $(CH_3COO)_2Mg$, 2 mM EDTA, 10 mM HEPES, pH 7.4, with NaOH and supplemented with protease inhibitors (10 mg/ml aprotinin, 2 mg/ml pepstatin A). To separate the membranes from cytosol, the postnuclear supernatant (PNS) was centrifuged at 80,000 × *g* for 20 min in a TLA 100.3 rotor using a Beckman Optima TL ultracentrifuge. The pellets were resuspended in homogenization buffer, loaded on the top of sucrose gradients (0.3–1.2 M sucrose), and then centrifuged at 110,000 × *g* for 30 min (velocity gradient). Fractions of 1 ml were collected from the top of the velocity gradients. 300 μl of each fraction from 4 to 8 were pooled and loaded on second sucrose gradients (1.1–2.0 M) and centrifuged at 110,000 × *g* for 18 h (equilibrium gradients). Equal aliquots (250 μl) of both gradient fractions and equal amounts of proteins of PNS prepared from wild type and NCS-1 cells were analyzed by Western blotting as described (18). Briefly, after electrophoresis, samples were electroblotted to nitrocellulose filters (Schleicher & Schuell) and probed with antibodies. The blots were then washed and incubated with the appropriate secondary antibodies conjugated to peroxidase. The peroxidase was detected using chemiluminescent substrate (Pierce). The levels of NCS-1 in the PNS were quantified by measuring the intensity of the bands in the autoradiograms using the analysis program Image 1.61 (National Technical Information Service, Springfield, VA).

Immunocytochemistry—Double immunofluorescence and confocal analysis on fixed cells were carried out as described (18). Briefly, the fixed cells were permeabilized with Triton X-100 and then incubated with the polyclonal anti-NCS-1 antibody and monoclonal antibodies against either synaptophysin or chromogranin B. After washing, the cells were incubated with the appropriate secondary antibodies conjugated to TRITC or fluorescein isothiocyanate, washed again, and mounted on glass coverslips with Mowiol. Images were collected in the MRC-1024 laser-scanning microscope (Bio-Rad) with ×40 or ×60 objective lenses. For comparison of double-stained patterns, images from the fluorescein isothiocyanate or TRITC channels were acquired independently from the same area of sample and then superimposed. Images were processed using Photoshop 4 (Adobe Systems, Mountain View, CA). Immunolabeling of frozen sections prepared from fixed and sucrose-embedded NCS-1 cells was performed as described (19). Monoclonal and polyclonal antibodies against the soluble granular proteins, chromogranin B and secretogranin II (SgII), were as previously described (19, 20). Anti-synaptophysin antibodies were obtained from Roche Molecular Biochemicals.

Ca^{2+} Imaging in Single Cells—Changes in $[Ca^{2+}]_i$ in single cells were measured by the fura-2 method as described by Grynkiewicz *et al.* (21) with minor modification (22). In brief, the culture medium was replaced with balanced salt solution of the following composition: 150 mM NaCl, 5.0 mM KCl, 1.8 mM $CaCl_2$, 1.2 mM $MgCl_2$, 25 mM HEPES, and 10 mM D-glucose, pH 7.4. Cells were loaded with fura-2 by incubation with 5 μM fura-2 acetoxymethylester (fura-2/AM) at room temperature (20–22 °C) in balanced salt solution for 30 min, followed by a balanced salt solution wash and a further 30-min incubation to allow de-esterification of the loaded dye. Then the coverslips were mounted on a microscope (TMD-300, Nikon, Tokyo, Japan) equipped with a xenon lamp and band pass filters of 340- and 360-nm wavelength. Image data, recorded by a high sensitivity silicon intensifier target camera (C-2741–08, Hamamatsu Photonics, Hamamatsu, Japan) were regulated by a Ca^{2+} analyzing system (Furusawa Laboratory Appliances).

Confocal Ca^{2+} Imaging—For recording subcellular Ca^{2+} signals, the cells were loaded with 5 μM fluo-3/AM for 30–40 min at room temperature. After a further 20–30 min for de-esterification of the acetoxymethyl ester, the coverslips were mounted on a microscope (E-600; Nikon, Tokyo, Japan) equipped with a CSU-10 laser-scanning unit (Yokogawa, Tokyo, Japan) and ICCD camera (C2400-87V; Hamamatsu Photonics). Fluo-3 was excited with the 488-nm line of an argon ion laser, and the emitted fluorescence was collected at wavelengths of >515 nm). A Nikon CFI Fluor ×60 water immersion objective (1.0 numerical aperture) was used. In order to compensate for uneven distribution of the fluo-3, self ratios were calculated ($R_s = F/F_0$), which were subsequently converted into Ca^{2+} concentration using the following equation.

$$[Ca^{2+}]_i = R_s * K_d / ((K_d / [Ca^{2+}]_{rest}) - R_s) \quad \text{(Eq. 1)}$$

The K_d value of fluo-3 for PC12 cells was taken to be 707 nM, which was determined by an *in vivo* calibration method (23).

Dopamine Release—The procedure for the measurement of released dopamine was the same as that described by Koizumi *et al.* (22). The

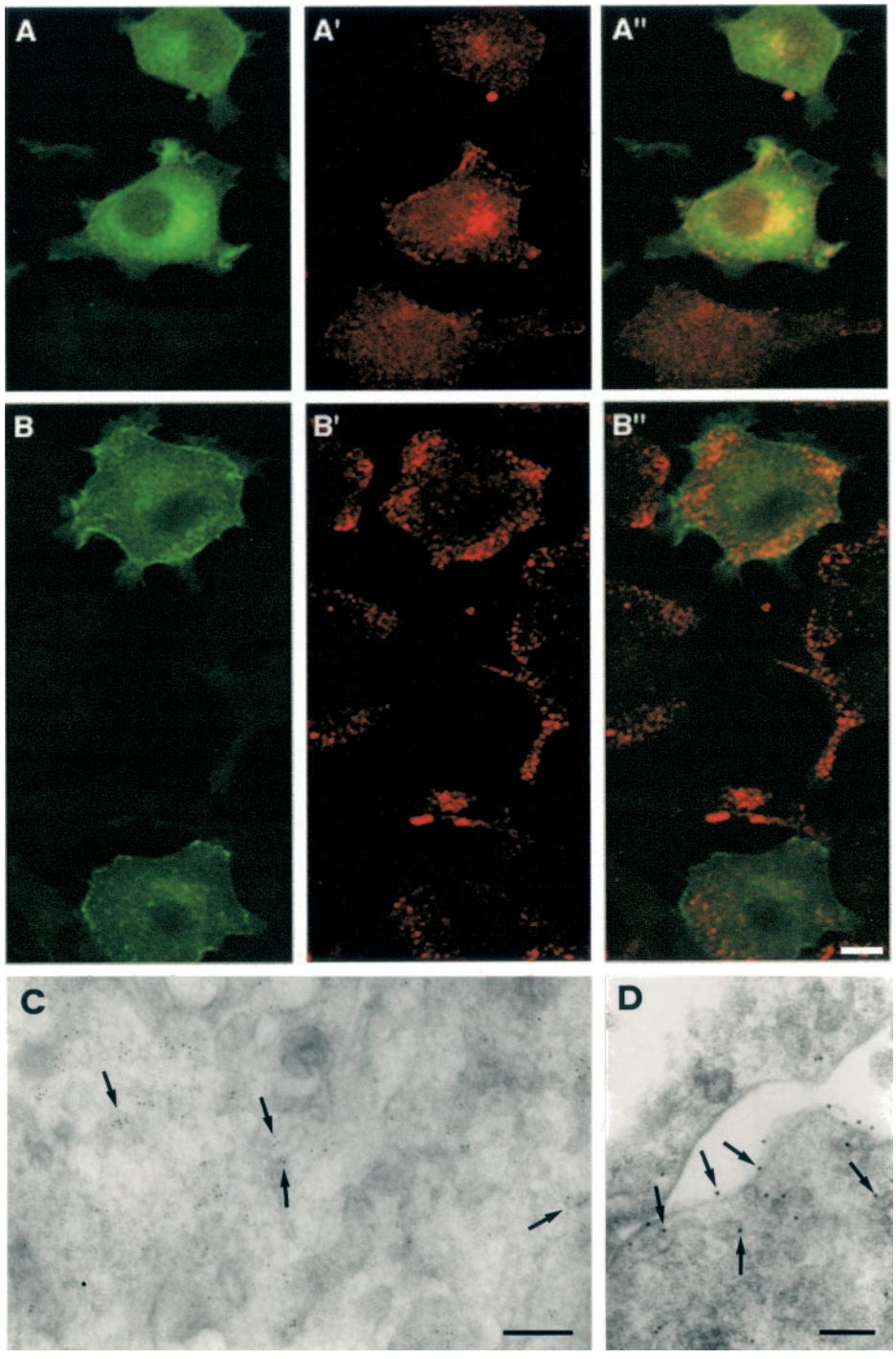

FIG. 2. **Immunocytochemical analysis of NCS-1.** *A–B″*, double immunofluorescence micrographs showing the distribution of NCS-1 in NCS-1 cells. After fixation, cells were double immunostained with anti-NCS-1 antibody (*A* and *B*) together with either anti-synaptophysin (*A′*) or anti-chromogranin B (*B′*) antibodies. *A″* and *B″*, superimposed images. Note a partial colocalization of NCS-1 with synaptophysin (*A″*; *yellow staining*). *Bar*, 10 μm. *C* and *D* show the subcellular localization of NCS-1. Ultrathin frozen sections of NCS-1 cells were immunolabeled with the anti-NCS-1 antibody followed by anti-rabbit IgG conjugated to 5-nm (*C*) or 10-nm (*D*) gold particles. The *arrows* indicate the presence of NCS-1 in small vesicle tubular structures (*C* and *D*) and the plasma membrane (*D*). *Bars*, 100 nm.

amount of dopamine released to superfusate and that remaining in the cells was determined by high performance liquid chromatography (HPLC) coupled with an electrochemical detector (LC-4B; Bioanalytical Systems, West Lafayette, IN). The percentage of release was calculated by dividing supernatant values by the sum of supernatant and pellet values.

Assay of Phosphoinositides and Inositol 1,4,5-Trisphosphate (Ins(1,4,5)P$_3$)—Subconfluent cells were labeled with *myo*-[^{3}H]inositol (3 μCi/ml) for 48 h and were equilibrated for 15 min in the presence of 10 mM LiCl before challenge with UTP. Incubations were terminated by the addition of an equal volume of 1 M trichloroacetic acid. The supernatant was recovered and neutralized, and [^{3}H]inositol phosphate ([^{3}H]InsP$_x$) accumulation was assessed as described previously (24). Cell residues were extracted with acidified chloroform/methanol to recover the total lipid fraction, and deacylation and separation of glycerophosphoinositol (phosphates) was performed (25). Experiments to measure changes in Ins(1,4,5)P$_3$ mass were performed as described above except that cells were not prelabeled with *myo*-[^{3}H]inositol, and LiCl was omitted from the medium (26).

RESULTS

Subcellular Localization of Endogenous and Recombinant NCS-1 in PC12 Cells—To determine the level of the expression and subcellular distribution of NCS-1, wild type or NCS-1-transfected PC12 cells were initially analyzed by immunoblotting and subcellular fractionation. Using a specific antibody, the levels of NCS-1 were analyzed in two different PC12 cell clones (clones 251 and N2) and in a number of stable transfected clones obtained from N2 cells (Fig. 1*A*). Whereas the level of endogenous NCS-1 was similar in the wild type clones, transfection with NCS-1 resulted in markedly enhanced levels of expression in a number of selected clones. The clone selected for further investigation (from here on referred to as NCS-1 cells) expressed ~6 times more NCS-1 than the wild type N2 cells.

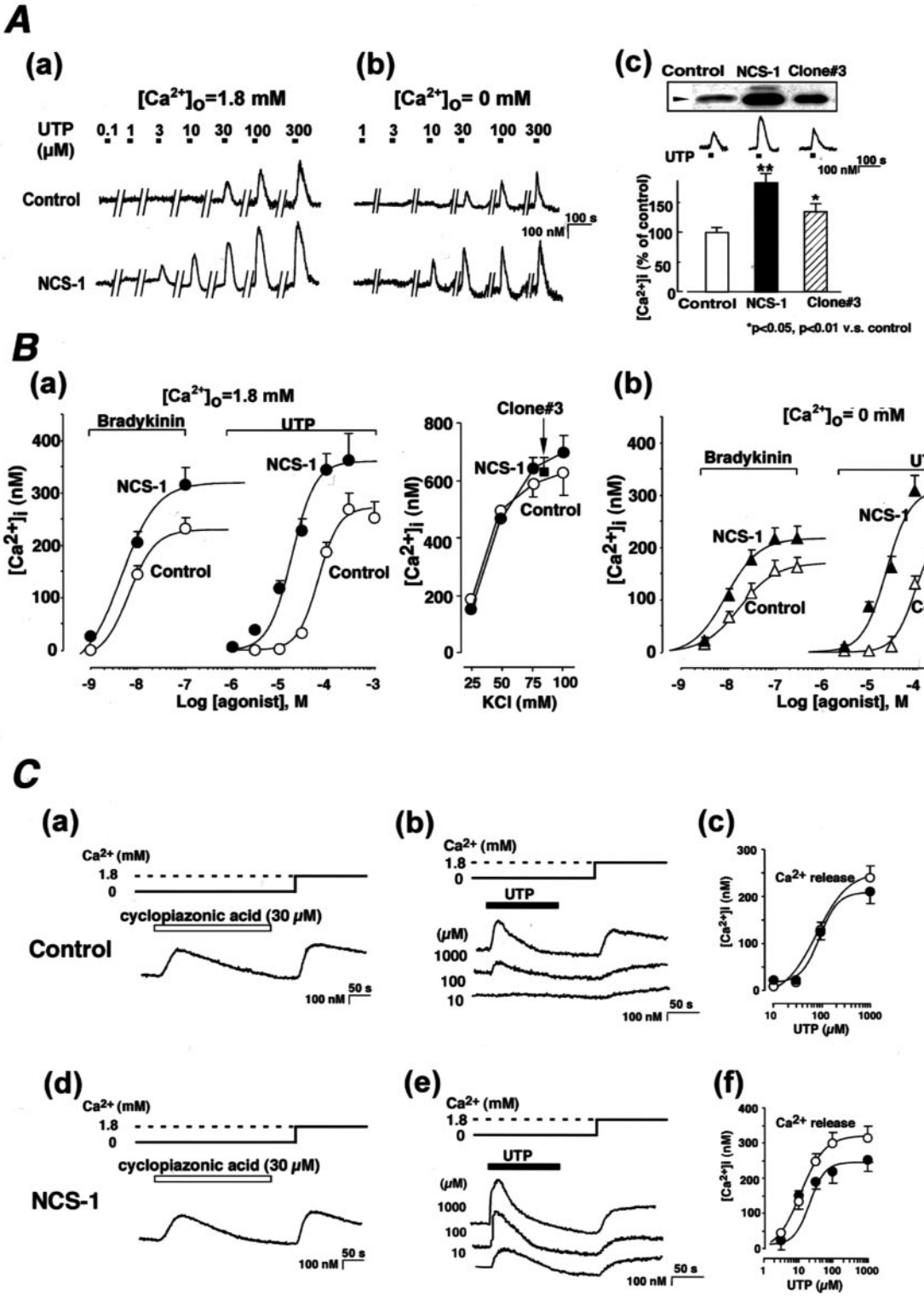

FIG. 3. **Concentration dependence of Ca^{2+} responses to UTP in NCS-1 cells compared with control cells.** *A*, *a* and *b*, typical Ca^{2+} responses to UTP in the presence and absence of $Ca^{2+}{}_o$, respectively. *Upper* and *lower traces* show Ca^{2+} responses in control and NCS-1 cells, respectively. The *traces* represent averaged responses from 32–56 cells. Cells were stimulated with various concentrations of UTP (0.1–300 μM) for 20 s separated by 5 min in the presence (*a*) and absence (*b*) of $Ca^{2+}{}_o$. *b*, Ca^{2+} (1.8 mM) was readmitted to the medium for 2 min between UTP stimulation to allow the stores to refill. *A* (*c*) shows the UTP-evoked elevation in $[Ca^{2+}]_i$ in another NCS-1-expressing clonal cell, clone 3 (with NCS-1 levels greater than control but less than that of NCS-1 cells). The *upper Western blotting panel* shows the level of NCS-1 in each clone. Typical traces of the UTP (100 μM)-evoked rises in $[Ca^{2+}]_i$ are shown just *below* the corresponding blot. The responses are summarized in the *bottom column*, which was normalized to the response of control cells. *B* (*a*) shows concentration-response curves for UTP-, bradykinin-, and high K^+-evoked elevation of $[Ca^{2+}]_i$ in control and NCS-1 cells. Similar to UTP, bradykinin (1–100 nM) was added to the cells for 20 s every 5 min. Ca^{2+} responses in control (*open circles*) and NCS-1 cells (*closed circles*) were plotted against the agonist concentration. The *closed square* shows high K^+-evoked $[Ca^{2+}]_i$ elevation in clone 3 cells. *B* (*b*) shows concentration-response curves for UTP- and bradykinin-evoked elevations of $[Ca^{2+}]_i$ in the clones in the absence of $Ca^{2+}{}_o$. The data are mean ± S.E. of 58–112 cells. Curves were fitted using a Hill equation. *C*, *a* and *d* illustrate typical traces of Ca^{2+} release evoked by cyclopiazonic acid (*horizontal open bars*) and Ca^{2+} entry evoked by the readdition of $Ca^{2+}{}_o$ in control (*a*) and NCS-1 cells (*d*). Cells were stimulated with cyclopiazonic acid (30 μM) for 4 min in the absence of $Ca^{2+}{}_o$ and washed by Ca^{2+}-free medium for another 1 min, and then $Ca^{2+}{}_o$ was readded. The traces represent averaged responses from 47 (*a*) and 51 (*d*) cells. *C*, *b* and *e* indicate typical traces of Ca^{2+}

Data from subcellular fractionation indicated a broad distribution of NCS-1 in transfected cells. As reported (5), a certain portion of NCS-1 was soluble in the cytosol. To study the distribution of the portion of protein associated with cellular organelles, the PNS were subjected to high speed centrifugation, and the pellets were resuspended in homogenization buffer. These were then analyzed by subcellular fractionation using two-step gradients. Analysis of the fractions obtained from the first (velocity) gradients, which separates organelles according to their size, revealed a broad distribution of NCS-1. In these velocity gradients, two peaks of NCS-1 were observed: one in the lighter fractions and the second in fractions 7–9 (Fig. 1*B*). This distribution is similar to that of synaptophysin, a protein present in the membrane of vesicles highly related to synaptic vesicles (referred to as synaptic-like microvesicles) (27) and known to recycle through the early endosomal compartment in PC12 cells (28, 29). A well known marker of the secretory granules, SgII (30), peaked in fractions 4–8, where some synaptophysin and NCS-1 were also present. In order to further analyze whether a portion of NCS-1 could be present in the membranes of secretory granules, aliquots of fractions 4–8 were collected and loaded on the equilibrium gradients in order to achieve separation of organelles according to their density. Western blotting analysis of the fractions from these gradients revealed the presence of NCS-1 mainly in the earlier fractions. This distribution was again very similar to that of synaptophysin. There was no colocalization of NCS-1 with the marker for secretory granules, SgII, which was in the denser fractions.

The cellular localization of NCS-1 in stably transfected PC12 cells was also studied by immunofluorescence and immunocytochemistry. As shown in Fig. 2, *A* and *B*, when NCS-1 cells were labeled with NCS-1 antibodies, intense immunofluorescence was seen in a large number of cells (about 60%). The immunostaining for NCS-1 was partially diffuse in the positive cells in agreement with its partial distribution in the cytosol (Fig. 2, *A* and *B*) (5). The anti-NCS-1 antibody also gave a punctate staining and showed partial colocalization with the immunostaining pattern of synaptophysin (see Fig. 2, *A–A″*). In contrast, very little colocalization was observed with the immunofluorescent pattern of chromogranin B, a well known marker for the secretory granules of PC12 cells (Fig. 2, *B–B″*). In addition, NCS-1 immunostaining was observed at the periphery of the positive cells, raising the possibility that a certain amount of the protein could be bound to the plasma membrane. To confirm this possibility, ultrathin frozen sections prepared from NCS-1 cells were immunolabeled with anti-NCS-1 antibodies and secondarily labeled with anti-rabbit IgG conjugated to 5-nm gold particles. As shown in Fig. 2, *C* and *D*, this revealed intracellular NCS-1 immunoreactivity, with gold particles distributed both in the cytoplasm and on small clear vesicles and tubules. In line with the immunofluorescence data, some gold particles were also found to decorate the plasma membrane, thus confirming the presence of NCS-1 at the cell surface in NCS-1 cells.

Enhancement by NCS-1 of Ca^{2+} Responses to UTP or Bradykinin—Stimulation of PC12 cells with the $P2Y_2$-selective agonist UTP results in the activation of phospholipase C (PLC) and the subsequent generation of Ins(1,4,5)P_3. Indeed, U73122 (10 μM), an inhibitor of PLC, substantially decreased the UTP-evoked elevation in intracellular Ca^{2+} concentration ($[Ca^{2+}]_i$) in the cells. In the presence of U73122, the UTP-evoked $[Ca^{2+}]_i$ was decreased by 93.3 ± 0.5% (n = 53 cells from two independent experiments). In PC12 cells, the normal consequence of UTP stimulation is the rapid release of Ca^{2+} from intracellular Ins(1,4,5)P_3-sensitive stores, followed by a more sustained Ca^{2+} entry across plasma membrane in response to store depletion (capacitative Ca^{2+} entry (CCE)) (31). In the current study, a brief UTP stimulation caused a transient pattern of $[Ca^{2+}]_i$ elevation consistent with Ca^{2+} mobilization and CCE in both vector-transfected control and NCS-1 cells in a concentration-dependent manner (Fig. 3*A*). However, UTP was significantly more potent in NCS-1 cells than in control cells (EC_{50} = 19 and 81 μM, respectively). Furthermore, the maximal $[Ca^{2+}]_i$ responses evoked by 300 μM UTP were significantly greater in NCS-1 cells than control cells (363 ± 52 nM *versus* 269 ± 31 nM, $p < 0.05$). The enhancement of Ca^{2+} responses was not a clonal artifact, because in another NCS-1-expressing clonal cell line (clone 3) whose NCS-1 levels are greater than control but less than that of NCS-1 cells, UTP was more potent than in control cells (Fig. 3*A*, *c*). Bradykinin also elevates $[Ca^{2+}]_i$ in PC12 cells via the PLC-coupled bradykinin B_2 receptor (32). Similar to the UTP-mediated responses, bradykinin elevated $[Ca^{2+}]_i$ in NCS-1 cells more potently than in control cells (EC_{50} values; 6.0 and 8.5 nM, respectively), and the maximal response was again enhanced (315 ± 34 nM *versus* 232 ± 21 nM, $p < 0.05$; 100 nM bradykinin) (Fig. 3*B*). This enhancement by NCS-1 of both UTP- and bradykinin-evoked Ca^{2+} signaling in NCS-1 cells was also apparent in the absence of extracellular Ca^{2+} ($Ca^{2+}{}_o$) (Fig. 3, *A* (*b*) and *B* (*b*)), indicating that the Ca^{2+} release process had itself been potentiated. U73122 (10 μM) also inhibited the Ca^{2+} responses to UTP in NCS-1 cells ($[Ca^{2+}]_i$ elevation was 5.3 ± 0.62% of that with UTP alone; n = 52 cells from two independent experiments). In contrast to these differences in UTP- and bradykinin-evoked responses between NCS-1 cells and control cells, the elevations in $[Ca^{2+}]_i$ evoked by depolarization with high K^+ (25–100 mM) were almost identical in control and NCS-1 cells (Fig. 3*B*, *a*).

To ascertain whether the CCE process *per se* was affected by NCS-1, we determined CCE directly in control and NCS-1 cells. CCE was activated by inhibiting the Ca^{2+}-ATPase of the endoplasmic reticulum using cyclopiazonic acid (30 μM). The elevations of $[Ca^{2+}]_i$ induced by cyclopiazonic acid were not different in control and NCS-1 cells (Fig. 3*C*, *a* and *d*; 117.2 + 16.5% of control, $p > 0.05$, n = 32 cells), indicating that CCE *per se* was unaffected by overexpression of NCS-1. We next monitored Ca^{2+} release and CCE separately to investigate the relationship between UTP-evoked Ca^{2+} release and Ca^{2+} entry. In the absence of $Ca^{2+}{}_o$, UTP produced concentration-dependent elevations of $[Ca^{2+}]_i$ in both control and NCS-1 cells (Fig. 3*C*, *b* and *e*). After the removal of UTP, readdition of $Ca^{2+}{}_o$ produced a sustained rise in $[Ca^{2+}]_i$, which slowly returned to basal levels after ~10 min. This rise was a consequence of CCE and was dependent upon the initial UTP concentration (Fig. 3*C*, *b*, *c*, *e*, and *f*). In other words, the extent of CCE is related to the extent of the UTP-mediated store depletion.

In addition to Ins(1,4,5)P_3 receptors, PC12 cells express functional type 2 ryanodine receptors on intracellular Ca^{2+} stores (33, 34). Activation of these Ca^{2+} release channels with 40 mM caffeine caused a rapid transient elevation in $[Ca^{2+}]_i$ of similar magnitude in control and NCS-1 cells (85.7 ± 19.2% of control,

release evoked by various concentrations of UTP (10–1000 μM, shown on the *left side* of each *trace*) in the absence of $Ca^{2+}{}_o$ and Ca^{2+} entry evoked by readdition of $Ca^{2+}{}_o$ in control (*b*) and NCS-1 cells (*e*). The *traces* represent averaged responses from 28–54 cells. Cells were stimulated with UTP for 2 min (*horizontal closed bars*) and washed by UTP-free/Ca^{2+}-free medium for another 1 min, and then Ca^{2+} (1.8 mM) was readded. Ca^{2+} responses in *C* (*b*) and *C* (*e*) are summarized in *C* (*c*) and *C* (*f*), respectively. The maximal Ca^{2+} release (*open circles*) and Ca^{2+} entry (*closed circles*) were plotted against the UTP concentration. The amplitude of initial Ca^{2+} release correlates to that of the subsequent Ca^{2+} entry in both clones. Curves were fitted using a Hill equation.

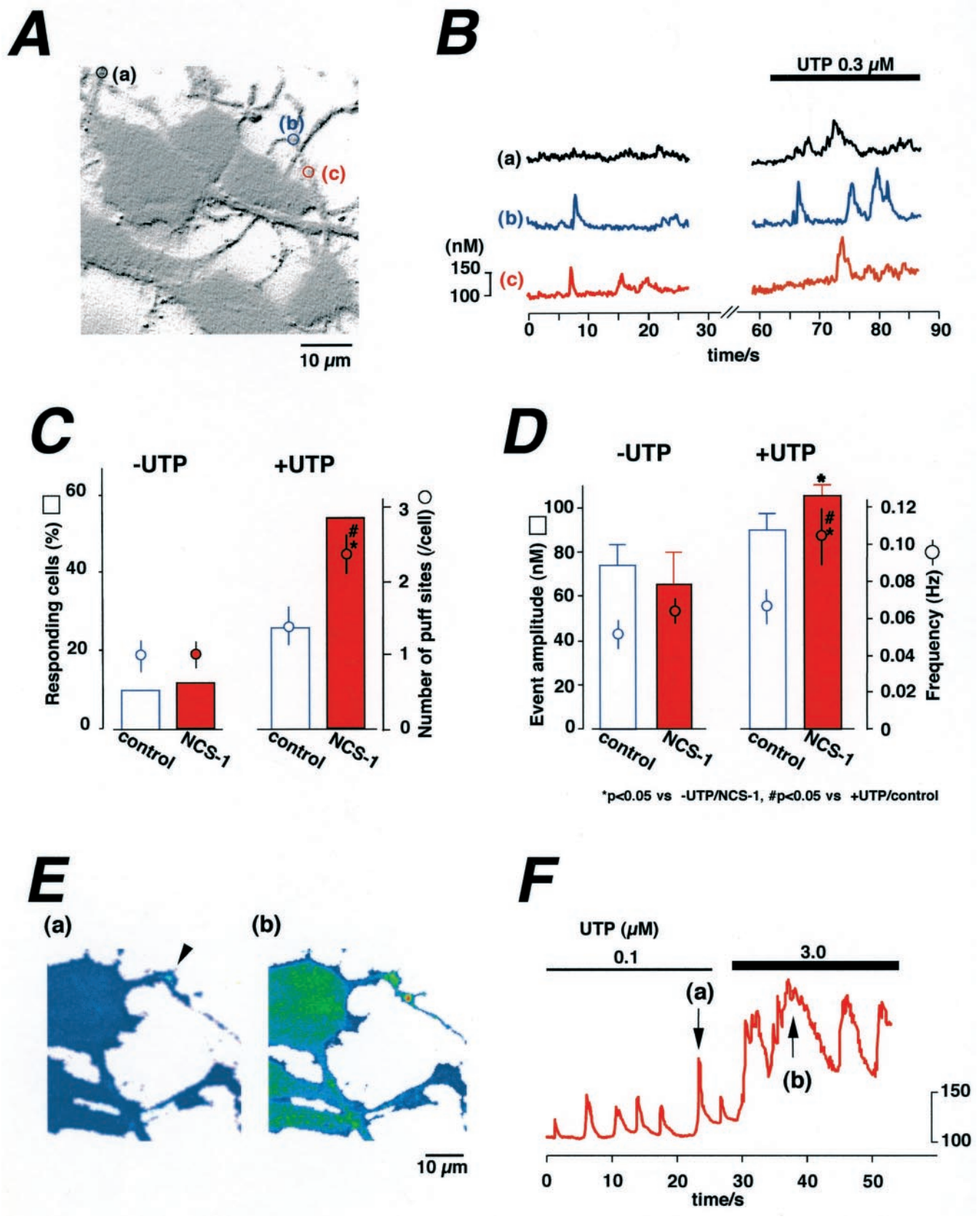

FIG. 4. **Characterization of elementary Ca^{2+} events in PC12 cells.** *A*, a phase-contrast image of NCS-1 cells. Each trace in *B* shows the time course of spontaneous and UTP (0.3 μM)-evoked changes in $[Ca^{2+}]_i$ at sites *a–c* in *A*. Characteristic features of these elementary Ca^{2+} release signals are summarized in *C* and *D*. In *C*, *bars* and *circles* indicate the fraction of cells that showed elementary Ca^{2+} release signals and the number of initiation sites for the elementary events (per cell) in the absence (−*UTP*) or presence of UTP (+*UTP*), respectively. In *D*, *bars* and *circles* show event amplitude and frequency of spontaneous or the UTP (0.3 μM)-evoked Ca^{2+} release events, respectively. The data are mean ± S.E. of 58–79 cells. Statistical analysis was performed by paired Student's *t* test. *E* (*a*) illustrates pseudocolor images of an elementary Ca^{2+} release event (*arrowhead*) evoked by 0.1 μM UTP in an NCS-1 cell. A higher UTP concentration (3 μM) applied subsequently resulted in a global Ca^{2+} response (E (*b*)). The time course of the UTP-evoked rise in $[Ca^{2+}]_i$ at the site indicated by the *arrowhead* in *E* is plotted in *F*.

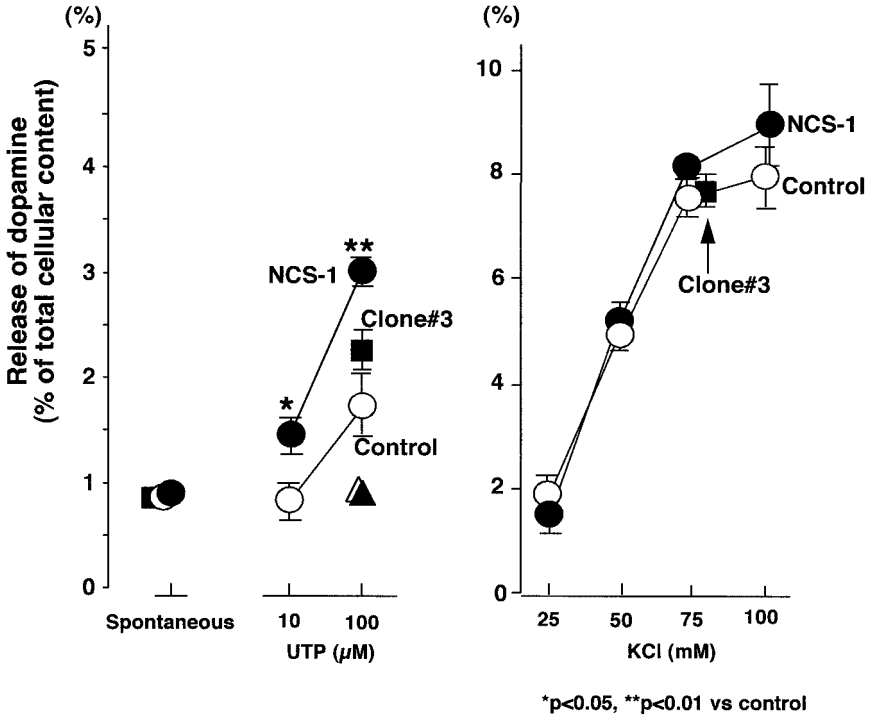

FIG. 5. **Enhancement of UTP-evoked secretion by NCS-1.** The HPLC assays of the UTP- and high K^+-evoked release of dopamine in the control, NCS-1, and clone 3 cells are shown. These are results from a typical experiment, with each data point being the mean ± S.E. of triplicate measurements. *Open circles*, *filled circles*, and *filled squares* show the responses in control cells, NCS-1 cells, and clone 3 cells, respectively. *Open* and *closed triangles* show the UTP (100 μM)-evoked dopamine release in the absence of $Ca^{2+}{}_o$ in control and NCS-1 cells, respectively. Three such experiments were performed and similar results were obtained. The release of dopamine is shown as a percentage of the total cellular content. Statistical analysis was performed by paired Student's *t* test.

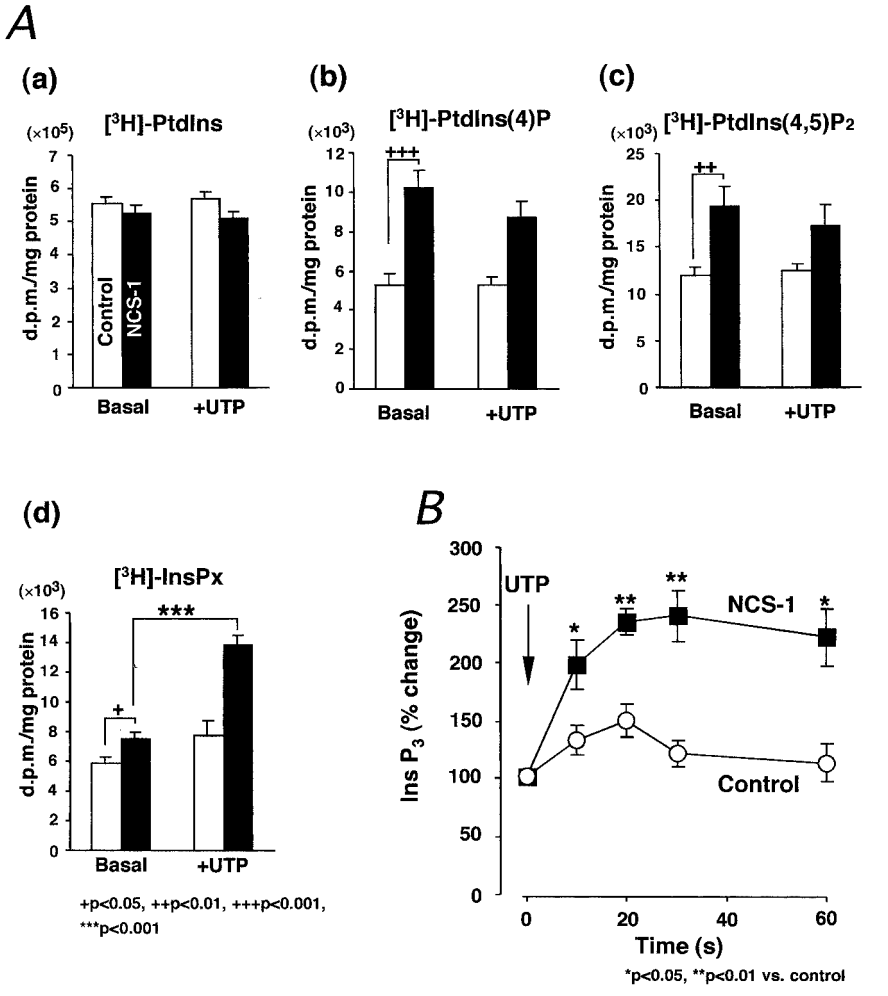

FIG. 6. **Comparison of the intracellular phosphoinositides levels in both clones.** *A*, *a–d* show intracellular concentrations of [^{3}H]PtdIns, [^{3}H]PtdIns(4)P, [^{3}H]PtdIns(4,5)P_2, and [^{3}H]InsP_x in the absence (*Basal*) and presence of 300 μM UTP (+*UTP*) in both clones. *Open* and *closed columns* show the amount of these phospholipids in vector control and NCS-1 cells, respectively. Cells were labeled with [^{3}H] inositol for 48 h and then stimulated with UTP for 60 s as described under "Experimental Procedures." Values shown are dpm/mg of protein. All data are presented as mean ± S.E. of seven experiments performed on three different days. Statistical significance is indicated as $p < 0.05$ (+), $p < 0.01$ (++), and $p < 0.001$ (+++) for basal NCS-1 cells *versus* vector control values and as $p < 0.001$ (***) for basal *versus* UTP stimulated values. *B*, time courses of UTP-evoked Ins(1,4,5)P_3 generation in control (*open circles*) and NCS-1 cells (*closed squares*). Ins(1,4,5)P_3 levels were determined by radioreceptor assay and expressed as percentage of basal levels which were 20.1 ± 3.6 and 24.1 ± 2.9 pmol/mg of protein for vector controls and NCS-1 cells, respectively. All data are mean ± S.E. of four independent experiments, each performed in duplicate. Statistical significance is shown as $p < 0.05$ (*) and $p < 0.01$ (**) for NCS-1 cells compared with vector control (Student's *t* test).

$n = 23$ cells from two independent experiments). Since we have reported that luminal [Ca^{2+}] affects the activity of both Ins(1,4,5)P_3 receptors and ryanodine receptors in PC12 cells (35, 36), the Ca^{2+} contents of the intracellular stores in control and NCS-1 cells were compared. In the absence of $Ca^{2+}{}_o$, ionomycin (5 μM) releases almost all Ca^{2+} from the intracellular

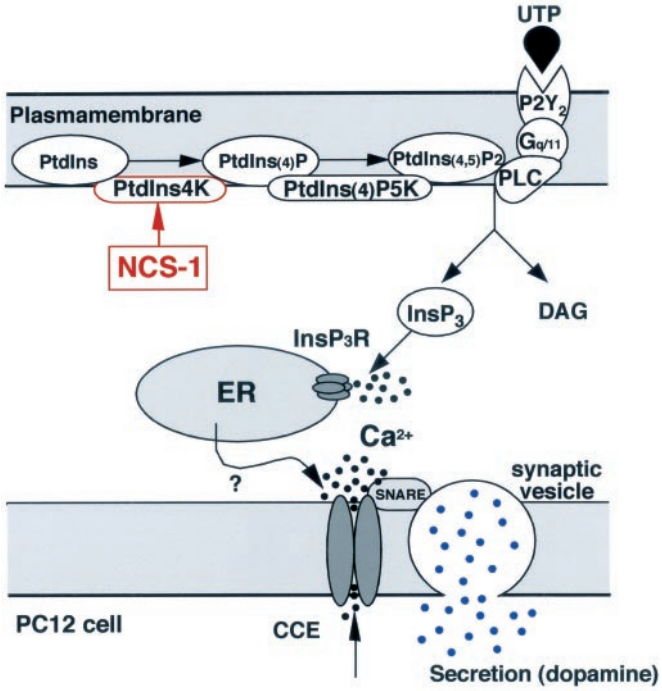

FIG. 7. **Diagram illustrating a working model for the regulation of Ca^{2+} signals and secretion by NCS-1 in PC12 cells.** See "Discussion" for details.

stores of PC12 cells (37). In NCS-1 cells, ionomycin-mediated elevations in $[Ca^{2+}]_i$ were similar to those in control cells (96.1 ± 6.3% of control, n = 32 cells from two independent experiments), indicating similar luminal Ca^{2+} contents in the two cell lines.

Elementary Ca^{2+} Release Events in NCS-1 Cells—Elementary Ca^{2+} release signals, such as puffs and sparks, are the building blocks for global Ca^{2+} signals (38, 39). Such elementary events have been observed in a wide variety of cell types including PC12 cells (35). Thus, using confocal microscopy, we investigated whether overexpression of NCS-1 affects elementary Ca^{2+} release events. Elementary Ca^{2+} signals were observed spontaneously (Fig. 4*B*, *left traces*), and these were facilitated upon stimulation with UTP concentrations (0.1 or 0.3 μM) that were subthreshold for global Ca^{2+} signaling. These elementary Ca^{2+} events were observed even in the absence of $Ca^{2+}{}_o$, suggesting that they were mainly due to Ca^{2+} release from Ca^{2+} stores. Low concentration (0.3 μM) of UTP increased both the number of responding cells and the number of active elementary Ca^{2+} release sites (Fig. 4*C*), and enhanced the event amplitude and frequency (Fig. 4*D*). When NCS-1 cells were stimulated with higher (*e.g.* 3 μM) concentrations of UTP, these elementary events were followed by global Ca^{2+} signals (Fig. 4, *E* and *F*). In control cells, spontaneous elementary Ca^{2+} events also occurred, but there were no significant differences with NCS-1 cells in either the proportion of cells in which events were observed or the event amplitude. However, in control cells, 0.3 μM UTP activated fewer additional elementary Ca^{2+} release sites in fewer cells. Furthermore, the frequency of UTP-stimulated elementary events was lower than that seen in NCS-1 cells. These data demonstrate that overexpression of NCS-1 enhanced elementary Ca^{2+} release events mediated by PLC-linked GPCRs, and as a consequence the NCS-1-expressing cells displayed global Ca^{2+} signals at low levels of stimulation.

NCS-1 Enhances Secretion Evoked by UTP but Not by High K^+—UTP evokes the release of dopamine from PC12 cells (31), and the effects of NCS-1 overexpression on UTP-evoked secretory responses were therefore investigated. The UTP-evoked release of dopamine into the superfusate was determined by HPLC. UTP caused the release of dopamine in a concentration-dependent manner in control and NCS-1 cells. At each UTP concentration, there was a significantly greater release of dopamine in NCS-1 cells compared with control cells (Fig. 5). We also examined the UTP-evoked release of dopamine in clone 3 cells (see Fig. 3*A*, *c*). The dopamine release by clone 3 cells was greater than control but less than that of NCS-1 cells. This UTP-evoked release of dopamine was dependent on $Ca^{2+}{}_o$ in all cell lines (Fig. 5, *triangles*). There was no significant difference in spontaneous or high K^+ (25–100 mM)-evoked dopamine release between control, NCS-1 and clone 3 cells. In addition, no significant difference was observed in total cellular dopamine content between the clones (control, 287.8 ± 22.6 (n = 9); NCS-1 cell, 291.6 ± 30.7 (n = 9) ng/dish; $p > 0.05$).

Enhancement of Phosphoinositide Signaling by NCS-1—Finally, the levels of various phosphoinositides in both clones were investigated (Fig. 6). Under basal conditions, there was no significant difference in [^{3}H]PtdIns levels between the two clones (Fig. 6*A*, *a*). In control cells, [^{3}H]phosphatidylinositol 4-phosphate (PtdIns(4)P) and [^{3}H]PtdIns(4,5)P_2 represented 1.0 and 2.2% of the total phosphoinositide pool, respectively. In NCS-1 cells, the levels of both PtdIns(4)P and PtdIns(4,5)P_2 were significantly increased to 2.2 and 3.7% of the total phosphoinositide pool, respectively (Fig. 6*A*, *a–c*). Stimulation of both clones with UTP (300 μM) resulted in accumulation of [^{3}H]InsP_x against a Li^+ block of inositol monophosphatase (Fig. 6*A*, *d*). The response to UTP was significantly enhanced in NCS-1 cells such that accumulation was greater (198% over basal at 20 min compared with 83% in vector controls) (Fig. 6*A*, *d*). UTP caused an increase in Ins(1,4,5)P_3 mass in control cells (Fig. 6*B*). There was a marked potentiation in the magnitude (228% over basal level at 20 s compared with 146% in vector controls) and the duration of the Ins(1,4,5)P_3 response to UTP in NCS-1 cells (Fig. 6*B*).

DISCUSSION

Subcellular Localization of NCS-1 and Implications for Its Functional Role—NCS-1 showed a broad subcellular localization in PC12 cells, being partially distributed in the cytoplasm and associated with vesicles and tubular-like structures. The morphological and biochemical results suggest that some NCS-1 may be associated with the membrane of the synaptic-like microvesicles. In contrast to previous observations (5), our results demonstrate that NCS-1 is mainly not associated with the membranes of secretory granules. Interestingly, NCS-1 is also associated with the plasma membrane. This localization may be consistent with the possible role of NCS-1 in the modulation of the function of plasma membrane channels and receptors (40), especially of voltage-gated Ca^{2+} channels (7–9). On the other hand, NCS-1 at the plasma membrane and on vesicle membranes may play an important role in the metabolism of phosphoinositides. This phospholipid family is involved in both signal transduction and also in vesicle formation from the plasma membrane, trans-Golgi network and endosomes (41). In yeast, the homologue of NCS-1 has been demonstrated to exist in a complex with and to activate the yeast PtdIns4K, phosphatidylinositol 4-OH kinase (1), and very recent data have shown a direct interaction of NCS-1 with PtdIns4K in eukaryotic cells as well (42). The membranous distribution of NCS-1 in the present study raises the possibility that NCS-1 may contribute to the activation and recruitment of PtdIns4K to the plasma membrane (or other organelles), allowing an increase of PtdIns metabolism and synthesis of the signaling molecule Ins(1,4,5)P_3, which therefore would affect subsequent

intracellular responses such as Ca^{2+} signaling and exocytosis (see Fig. 7).

Overexpression of NCS-1 Enhances Elementary and Global Ca^{2+} Signaling and Secretory Responses—PC12 cells express both voltage- (43) and ligand-gated channels (44) through which Ca^{2+} entry is able to evoke exocytosis. Of particular relevance to the current study, PC12 cells express $P2X_2$ nonselective cation channels (45). Although ATP effectively activates this receptor, UTP evokes little (0–6% of the maximal ATP response) (46) or no (45) current through this channel. UTP-mediated $[Ca^{2+}]_i$ responses in these cells can therefore be considered to be mediated via activation of PLC-coupled, $P2Y_2$ receptors. Despite the ability of UTP to elevate $[Ca^{2+}]_i$ in the absence of $Ca^{2+}{}_o$, the effects of UTP on exocytosis were totally dependent upon $Ca^{2+}{}_o$. We demonstrated that the entry of Ca^{2+} across the plasma membrane is a consequence of CCE and that its magnitude is dependent upon the amplitude of the UTP-evoked elevation of $[Ca^{2+}]_i$ (as an index of the extent of store depletion). Thus, CCE, in response to the depletion of intracellular Ca^{2+} stores, links the activation of PLC-coupled $P2Y_2$ receptors to exocytotic events in PC12 cells. The findings that bradykinin-evoked release of [^{3}H]noradrenaline from PC12 cells was largely inhibited either by the removal of $Ca^{2+}{}_o$ or by the addition of SK&F96365, an inhibitor of CCE (47) and that caffeine-mediated release of Ca^{2+} from intracellular stores via ryanodine receptors triggers secretion from PC12 cells in a manner dependent upon $Ca^{2+}{}_o$ (34, 48) further support the role of CCE in exocytosis.

NCS-1 did not influence depolarization (high K^+)-evoked exocytosis, supporting a previous observation that Ca^{2+} sensitivity of the exocytotic process is not affected by NCS-1 overexpression (5). In addition, the effect of NCS-1 on voltage-gated Ca^{2+} channels in PC12 cells appears to be negligible. The ability of NCS-1 to enhance exocytosis in PC12 cells therefore implies that this protein enhances CCE. However, CCE resulting from store depletion by inhibition of the endoplasmic reticulum Ca^{2+}-ATPase with cyclopiazonic acid was unaffected. Furthermore, there was no difference in stored Ca^{2+} contents or in responses to caffeine between the clones (see "Results"). These data demonstrate that the CCE mechanism *per se* was not potentiated by NCS-1 overexpression and indicate that NCS-1 exerts its effects on secretion through enhanced GPCR-mediated Ca^{2+} release from intracellular stores. Our data are fully in accord with this hypothesis and demonstrate that overexpression of NCS-1 enhances elementary and global Ca^{2+} signaling in response to GPCR activation. Although the amplitudes of the initial, transient agonist-mediated global Ca^{2+} signaling events were in excess of the more sustained elevation due to CCE, the former were unable to evoke exocytosis. This is in agreement with previous studies demonstrating that CCE in response to depletion of either $Ins(1,4,5)P_3$- or ryanodine-sensitive stores triggers exocytosis more efficiently than the Ca^{2+} release process (31, 34, 48, 49). The reason for this is unclear. The exocytotic Ca^{2+} sensors appear to possess a low affinity for Ca^{2+}, requiring 10–100 μM for activation (50, 51). Although global measurements following depolarization reveal $[Ca^{2+}]_i$ on the order of 1 μM in many cell types, it is believed that much higher local $[Ca^{2+}]_i$ is achieved in subplasmalemmal microdomains due to the spatial packing of voltage-gated Ca^{2+} channels (52, 53). It is likely, therefore, that the spatial arrangement of Ca^{2+} channels (*e.g.* CCE channels and $Ins(1,4,5)P_3$ receptors) and the exocytotic machinery dictate whether Ca^{2+} fluxes are able to regulate vesicular release.

Overexpression of NCS-1 also enhanced the elementary Ca^{2+} release events. Such elementary Ca^{2+} signals were brief (lifetime ~1 s) $[Ca^{2+}]_i$ increases with a spatial spread of ~3–6 μm. In control cells, the amplitudes of the elementary events typically ranged from 80 to 100 nM, and the frequency was generally less than 0.1 Hz (0.06–0.1 Hz). All of these characteristic features are well in accord with elementary Ca^{2+} events previously described in nerve growth factor-differentiated PC12 cells (35). Without stimulation (−UTP), there was little difference in the characteristics of elementary Ca^{2+} release events between control and NCS-1 cells. However, upon stimulation with UTP, the number of cells showing elementary Ca^{2+} signals increased, as did the number of active elementary Ca^{2+} release sites within individual cells. In addition, the frequency of the events was dramatically enhanced. Global Ca^{2+} signals arise via the coordinated recruitment of elementary Ca^{2+} release sites (35, 39, 54). The potentiation of elementary Ca^{2+} signaling in NCS-1 cells therefore underlies their propensity to show global Ca^{2+} signals with low UTP concentrations.

Overexpression of NCS-1 Increases the Level of Polyphosphoinositides and Facilitates Agonist-mediated $Ins(1,4,5)P_3$ Production—Varieties of mechanisms have been proposed to account for the role of NCS-1 in synaptic enhancement and in exocytosis. Probable explanations for the NCS-1-evoked enhancement may be due to modulation of ion channels such as voltage-gated Ca^{2+} channels (7–9) and A-type K^+ channels (10). Recently, NCS-1 has been identified as an upstream activator of a specific isoform of PtdIns4K, phosphatidylinositol 4-OH kinase, in yeast (1). Here we demonstrated that in PC12 cells vertebrate NCS-1 significantly increased the levels of both PtdIns(4)P and $PtdIns(4,5)P_2$ without affecting those of PtdIns and facilitated $Ins(1,4,5)P_3$ production in response to UTP, an agonist to PLCβ-linked GPCRs. We therefore propose the following model for mechanisms that may underlie the enhancement by NCS-1 of exocytosis (see Fig. 7). First, NCS-1 binds to PtdIns4K located on the plasma membrane (or synaptic vesicles) and up-regulates its activity. This is followed by an increase in the local production of PtdIns(4)P and $PtdIns(4,5)P_2$, which serves as substrate for PLC, resulting in an increase in the production of $Ins(1,4,5)P_3$ and diacylglycerol in response to UTP (or bradykinin). This local increase in $Ins(1,4,5)P_3$ evokes elementary and global Ca^{2+} responses including both Ca^{2+} release via the $Ins(1,4,5)P_3$ receptor and CCE, leading to an enhancement of the secretory response. The dynamics of the interaction between PtdIns4K and NCS-1 remain to be investigated in detail. The fact that the interaction and activation of phosphatidylinositol 4-OH kinase/PtdIns4K is dependent on the myristoylation of NCS-1 suggests that the interaction should occur in a membranous environment. NCS-1, which is also present on the synaptic vesicle fraction, could translocate to the plasma membrane upon stimulation and thereby either recruit PtdIns4K to the plasmamembrane or activate preexisting PtdIns4K (55). The stable PC12 cells now allow us to address these issues.

In summary, we have for the first time demonstrated a role of mammalian NCS-1, as an important member of this family of EF-hand of Ca^{2+}-binding proteins, in phosphoinositide turnover, Ca^{2+} signaling, and exocytosis. We have presented evidence that NCS-1 enhances exocytosis by increasing Ca^{2+} signaling, which involves enhanced generation of $Ins(1,4,5)P_3$. This is a novel regulatory mechanism of exocytosis that might involve the activation of PtdInd4K. The revealed regulatory mechanisms would provide the basis to study their importance in other neurosecretory cells such as chromaffin cells or neurons.

Acknowledgments—We thank Rajendra Mistry and Tomoko Obama for the excellent technical assistance and Dr. Yasuo Ohno for continuous encouragement.

REFERENCES

1. Hendricks, K. B., Wang, B. Q., Schnieders, E. A., and Thorner, J. (1999) *Nat. Cell Biol.* **1,** 234–241
2. Allen, R. D., Al-Harbi, I. S., Morris, J. G., Clouston, P. D., O'Connell, P. J., Chapman, J. R., and Nankivell, B. J. (1997) *Transplantation* **63,** 830–838
3. Pongs, O., Lindemeier, J., Zhu, X. R., Theil, T., Engelkamp, D., Krah-Jentgens, I., Lambrecht, H. G., Koch, K. W., Schwemer, J., and Rivosecchi, R. (1993) *Neuron* **11,** 15–28
4. Olafsson, P., Wang, T., and Lu, B. (1995) *Proc. Natl. Acad. Sci. U. S. A.* **92,** 8001–8005
5. McFerran, B. W., Graham, M. E., and Burgoyne, R. D. (1998) *J. Biol. Chem.* **273,** 22768–22772
6. McFerran, B. W., Weiss, J. L., and Burgoyne, R. D. (1999) *J. Biol. Chem.* **274,** 30258–30265
7. Weiss, J. L., Archer, D. A., and Burgoyne, R. D. (2000) *J. Biol. Chem.* **275,** 40082–40087
8. Wang, C. Y., Yang, F., He, X., Chow, A., Du, J., Russell, J. T., and Lu, B. (2001) *Neuron* **32,** 99–112
9. Tsujimoto, T., Jeromin, A., Saitoh, N., Roder, J. C., and Takahashi, T. (2002) *Science* **295,** 2276–2279
10. Nakamura, T. Y., Pountney, D. J., Ozaita, A., Nandi, S., Ueda, S., Rudy, B., and Coetzee, W. A. (2001) *Proc. Natl. Acad. Sci. U. S. A.* **98,** 12808–12813
11. De Castro, E., Nef, S., Fiumelli, H., Lenz, S. E., Kawamura, S., and Nef, P. (1995) *Biochem. Biophys. Res. Commun.* **216,** 133–140
12. Iacovelli, L., Sallese, M., Mariggio, S., and de Blasi, A. (1999) *FASEB J.* **13,** 1–8
13. Schaad, N. C., De Castro, E., Nef, S., Hegi, S., Hinrichsen, R., Martone, M. E., Ellisman, M. H., Sikkink, R., Rusnak, F., Sygush, J., and Nef, P. (1996) *Proc. Natl. Acad. Sci. U. S. A.* **93,** 9253–9258
14. Bartlett, S. E., Reynolds, A. J., Weible, M., Jeromin, A., Roder, J., and Hendry, I. A. (2000) *J. Neurosci. Res.* **62,** 216–224
15. Inoue, K., and Kenimer, J. G. (1988) *J. Biol. Chem.* **263,** 8157–8161
16. Tooze, S. A., and Huttner, W. B. (1990) *Cell* **60,** 837–847
17. Passafaro, M., Rosa, P., Sala, C., Clementi, F., and Sher, E. (1996) *J. Biol. Chem.* **271,** 30096–30104
18. Rowe, J., Corradi, N., Malosio, M. L., Taverna, E., Halban, P., Meldolesi, J., and Rosa, P. (1999) *J. Cell Sci.* **112,** 1865–1877
19. Calegari, F., Coco, S., Taverna, E., Bassetti, M., Verderio, C., Corradi, N., Matteoli, M., and Rosa, P. (1999) *J. Biol. Chem.* **274,** 22539–22547
20. Rosa, P., Weiss, U., Pepperkok, R., Ansorge, W., Niehrs, C., Stelzer, E. H., and Huttner, W. B. (1989) *J. Cell Biol.* **109,** 17–34
21. Grynkiewicz, G., Poenie, M., and Tsien, R. Y. (1985) *J. Biol. Chem.* **260,** 3440–3450
22. Koizumi, S., Ikeda, M., Inoue, K., and Nakazawa, K. (1995) *Brain Res* **673,** 75–82
23. Thomas, D., Tovey, S. C., Collins, T. J., Bootman, M. D., Berridge, M. J., and Lipp, P. (2000) *Cell Calcium* **28,** 213–223
24. Challiss, R. A. J., Jenkinson, S., Mistry, R., Batty, I. H., and Nahorski, S. R. (1993) *Neuroprotocols* **3,** 135–144
25. Chilvers, E. R., Batty, I. H., Challiss, R. A., Barnes, P. J., and Nahorski, S. R. (1991) *Biochem. J.* **275,** 373–379
26. Challiss, R. A., Batty, I. H., and Nahorski, S. R. (1988) *Biochem. Biophys. Res. Commun.* **157,** 684–691
27. Thomas-Reetz, A. C., and De Camilli, P. (1994) *FASEB J.* **8,** 209–216
28. Cameron, P. L., Sudhof, T. C., Jahn, R., and De Camilli, P. (1991) *J. Cell Biol.* **115,** 151–164
29. Clift-O'Grady, L., Linstedt, A. D., Lowe, A. W., Grote, E., and Kelly, R. B. (1990) *J. Cell Biol.* **110,** 1693–1703
30. Huttner, W. B., Gerdes, H. H., and Rosa, P. (1991) *Trends Biochem. Sci.* **16,** 27–30
31. Koizumi, S., Nakazawa, K., and Inoue, K. (1995) *Br. J. Pharmacol.* **115,** 1502–1508
32. Appell, K. C., and Barefoot, D. S. (1989) *Biochem. J.* **263,** 11–18
33. Bennett, D. L., Bootman, M. D., Berridge, M. J., and Cheek, T. R. (1998) *Biochem. J.* **329,** 349–357
34. Koizumi, S., and Inoue, K. (1998) *Biochem. Biophys. Res. Commun.* **247,** 293–298
35. Koizumi, S., Bootman, M. D., Bobanovic, L. K., Schell, M. J., Berridge, M. J., and Lipp, P. (1999) *Neuron* **22,** 125–137
36. Koizumi, S., Lipp, P., Berridge, M. J., and Bootman, M. D. (1999) *J. Biol. Chem.* **274,** 33327–33333
37. Fasolato, C., Zottini, M., Clementi, E., Zacchetti, D., Meldolesi, J., and Pozzan, T. (1991) *J. Biol. Chem.* **266,** 20159–20167
38. Berridge, M. J. (1997) *J. Physiol.* **499,** 291–306
39. Bootman, M. D., Berridge, M. J., and Lipp, P. (1997) *Cell* **91,** 367–373
40. Nef, S., Fiumelli, H., de Castro, E., Raes, M. B., and Nef, P. (1995) *J. Recept. Signal Transduct. Res.* **15,** 365–378
41. De Camilli, P., Emr, S. D., McPherson, P. S., and Novick, P. (1996) *Science* **271,** 1533–1539
42. Pan, C.-Y., Jeromin, A., Lundstrom, K., Yoo, S. H., Roder, J., and Fox, A. P. (2002) *J. Neurosci.* **22,** 2427–2433
43. Di Virgilio, F., Milani, D., Leon, A., Meldolesi, J., and Pozzan, T. (1987) *J. Biol. Chem.* **262,** 9189–9195
44. Inoue, K., Nakazawa, K., Fujimori, K., and Takanaka, A. (1989) *Neurosci. Lett.* **106,** 294–299
45. Brake, A. J., Wagenbach, M. J., and Julius, D. (1994) *Nature* **371,** 519–523
46. Evans, R. J., Lewis, C., Buell, G., Valera, S., North, R. A., and Surprenant, A. (1995) *Mol. Pharmacol.* **48,** 178–183
47. Kim, Y. H., Park, T. J., Lee, Y. H., Baek, K. J., Suh, P. G., Ryu, S. H., and Kim, K. T. (1999) *J. Biol. Chem.* **274,** 26127–26134
48. Taylor, S. C., and Peers, C. (1999) *J. Neurochem.* **73,** 874–880
49. Taylor, S. C., and Peers, C. (2000) *J. Neurochem.* **75,** 1583–1589
50. Brose, N., Petrenko, A. G., Sudhof, T. C., and Jahn, R. (1992) *Science* **256,** 1021–1025
51. Heinemann, C., Chow, R. H., Neher, E., and Zucker, R. S. (1994) *Biophys. J.* **67,** 2546–2557
52. Llinas, R., Sugimori, M., and Silver, R. B. (1992) *Science* **256,** 677–679
53. Smith, S. J., Buchanan, J., Osses, L. R., Charlton, M. P., and Augustine, G. J. (1993) *J. Physiol.* **472,** 573–593
54. Marchant, J., Callamaras, N., and Parker, I. (1999) *EMBO J.* **18,** 5285–5299
55. Meyer, T., and York, J. D. (1999) *Nat. Cell Biol.* **1,** E93–E95